Electronic Supplementary Material (ESI) for Nanoscale.
This journal is © The Royal Society of Chemistry 2016

Search for effective chemical quenching to arrest molecular assembly and directly monitor DNA nanostructure formation

Jacob M. Majikes, Jessica A. Nash and Thomas H. LaBean

Figure S1 Shows the five potential quenching agents we identified and examined in this study, formaldehyde, glutaraldehyde, epichlorohydrin, 8-methoxy psoralen (8MOP), and streptozotocin. It has been established in the literature that formaldehyde, epichlorohydrin and 8MOP all can create crosslinks on AT/TA nucleobase sequences.[1,2]

8MOP was tested first as it has been used to crosslink DNA origami.[2] As per previous DNA origami crosslinking studies, 8MOP was dissolved in DMSO at high concentration, then added to samples, followed by exposure to UVA light for 1 hr. DNA origami samples were treated at high temperature, 80°C, in a heating block, then were allowed to slowly cool. 8MOP was added to concentration equivalent to the Ragendran work for 15 nM circle miniOrigami.[2] This failed to prevent origami formation, and was repeated with enough 8MOP that a small amount precipitated on being mixed into aqueous solution with the origami sample. Figure S2 shows this sample, and visibly contains many fully formed circle nanostructures.

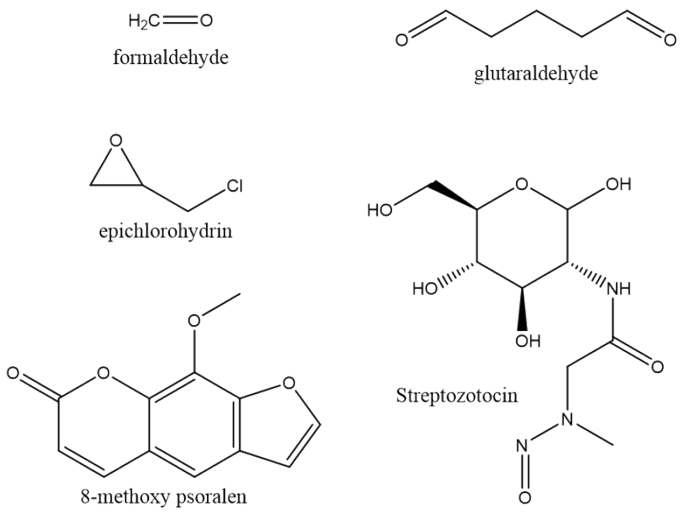

Figure S1. *Potential chemical quench candidates*

As origami formed in the samples shown in Figure S2, 8MOP does not appear to prevent DNA origami formation at 15 nM miniM13, equivalent to 5 nM M13.

After removing 8MOP from consideration, the remaining four candidates were evaluated in parallel via gel electrophoresis. Aliquots of 5 nM Tall Rectangle were treated with 1x, 20x, 100x, 500x, 1000x, and 3000x equivalents of a candidate, relative to the number of nucleotides in a 5 nM M13 anneal with a standard 10x staple excess. Each aliquot of TR was 15 µL in volume, and the candidates were added in 7.5 µL volumes as described in the methods section. The candidates were added at 56°C and allowed to incubate for 5 minutes before allowing the continuous thermal anneal to resume. The TR was used as miniM13 structures show minimal differences in electrophoretic migration for the scaffold, partially formed, and fully formed origami (Figure S3)These candidates were compared, in Figure S3, to TR quenched via liquid nitrogen at 56°C. From Figure S3, it is clear that both epichlorohydrin and streptozotocin do not appear to change migration within this range of excess quencher. Streptozotocin is known to have temperature dependent hydrolysis in water, [3] and was thus not pursued further. As at least one candidate (streptozotocin) was removed from consideration, formaldehyde, glutaraldehyde and epichlorohydrin were all moved forward.

To further examine the formaldehyde, glutaraldehyde, and epichlorohydrin, chemical and liquid nitrogen quenches were performed over a broad temperature range, with gel images shown in Figure S4. All of the chemical quenches in Figure S4 were performed at 500x, as at 500x both formaldehyde and glutaraldehyde had a similar band migration to the liquid nitrogen quench. The disappearance of the epichlorohydrin bands above 54°C is likely due to

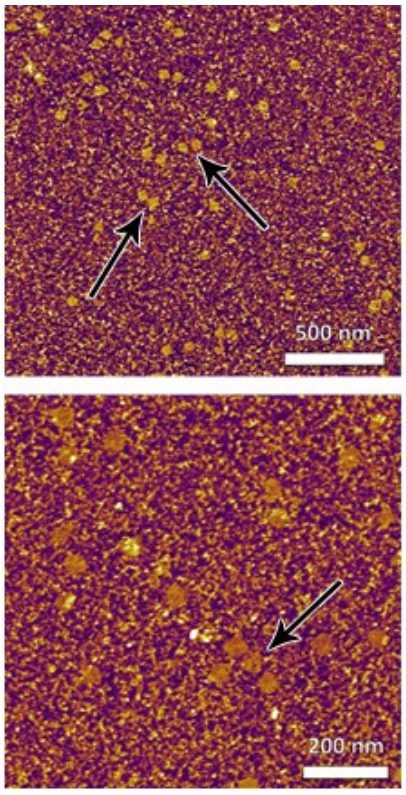

Figure S2. *Initial 8MOP test 15 nM circle miniM13 origami treated with 8MOP at*

chemical degradation of the DNA. Given the similarities between the liquid nitrogen quench and the aldehyde quenches, epichlorohydrin was not pursued further.

To further pursue glutaraldehyde and formaldehyde as quenchers, large samples of 56°C quenches were made for liquid nitrogen, formaldehyde and glutaraldehyde. All three were gel purified to allow comparison, with gels and AFM images shown in Figure S5. The formaldehyde quench appears quite similar to the primary, brighter, band of the liquid nitrogen quench. The glutaraldehyde quench does not appear to be similar to the liquid nitrogen quench, and in general is more completely formed than either the liquid nitrogen or formaldehyde quenches, as one would anticipate from the gel images in Figure S4.

This, combined with the gradual transition in the glutaraldehyde samples in Figure S4, contrasted with the rapid transition for the liquid nitrogen quench, glutaraldehyde was not pursued further. It is possible that glutaraldehyde could be effective at a different excess or incubation times.

As shown in Figure S3, when quenched at a constant excess of formaldehyde (500x) over a broad temperature range, it is clear that at higher temperatures the nanostructure is being partially denatured. Assuming Arrhenius behavior, one would expect exponential increases in the formaldehyde reaction rate with temperature. In order to offset this, the formaldehyde excess could be varied with the temperature at which it is being added.

Rearrangement of the Arrhenius function to solve for the concentration of quencher while holding the DNA concentration, reaction time, and overall reaction rate, constant results in an exponential function. As such, the minimum excess of formaldehyde relative to DNA was fitted to an exponential function.

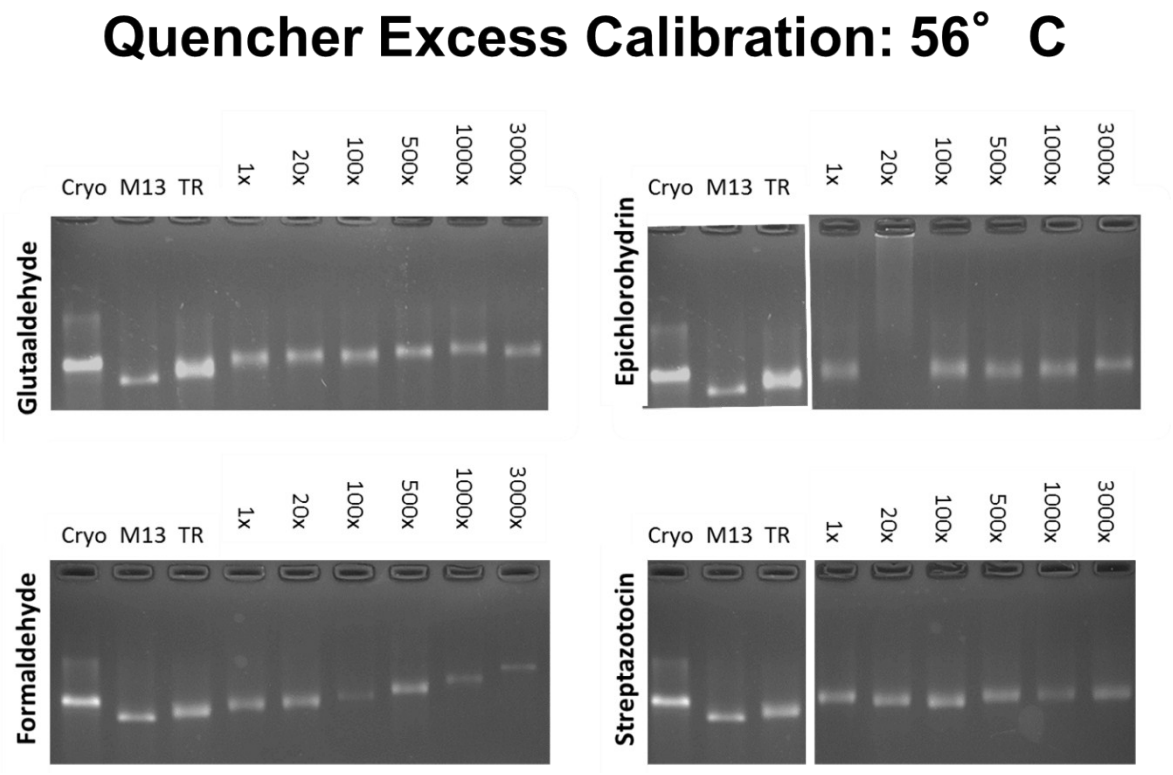

Figure S3. *Gel images for each quencher candidate with increasing excesses of potential quenchers. Each compares the liquid nitrogen quench (cryo), M13 scaffold, and fully formed Tall Rectangle (TR) to six samples which have increasing excesses of a quencher candidate, relative to the total number of nucleotides in the sample.*

The gel shown in Figure S4 show the quenching of two complementary strands using different excesses of

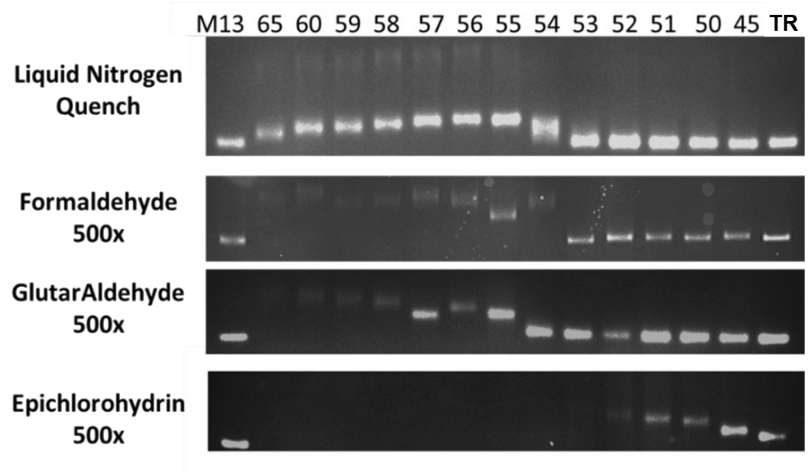

Figure S4. *Gel electrophoresis images for TR quenches at various temperatures during continuous thermal annealing. Gradients for liquid nitrogen, formaldehyde, glutaraldehyde and epichlorohydrin are compared. with 500x formaldehyde having the closes shift to the liquid nitrogen quench.*

formaldehyde at 65°C and 50°C. Increased intensities at the ssDNA band or decreased intensity in the dsDNA band indicate the ssDNA had been rendered inert prior to hybridization at ~40°C. From this it is clear that >200x formaldehyde would be required to effectively quench at 65°C. For fitting we used 250x as the ssDNA band was increasingly strong as the excesses led to 200x for 65°C. At 50°C ~750x was clearly sufficient for quenching. From the gels in Figure 3, it is reasonable to consider 500x sufficient for quenching at 56°C. These were fitted to the exponential function, which was then used to perform quenches in Figure 5. MiniM13 structure quenches performed with at static 500x formaldehyde excess resulted in an almost immediate transition between fully formed and fully denatured, preventing study of intermediate states. As such, varying the formaldehyde excess was clearly beneficial, if not a complete solution.
Equation 1, was the result of the fitting, in which T is the temperature in Celsius. To account for changes in concentration, Equation 2 was used to ensure constant time to reaction completion.

Eq. 1: $Minimum\ Excess\ (5\ nM\ M13\ origami, 10x\ Staples) \approx\ 1E^{-}5e^{9496/T+273}$

Eq. 2: $Minimum\ Excess\ (Conc) = X(5\ nM)\frac{5\ nM}{Conc}$

These equations provide a very rough first estimate for varying the relative excess of formaldehyde as a function of temperature.

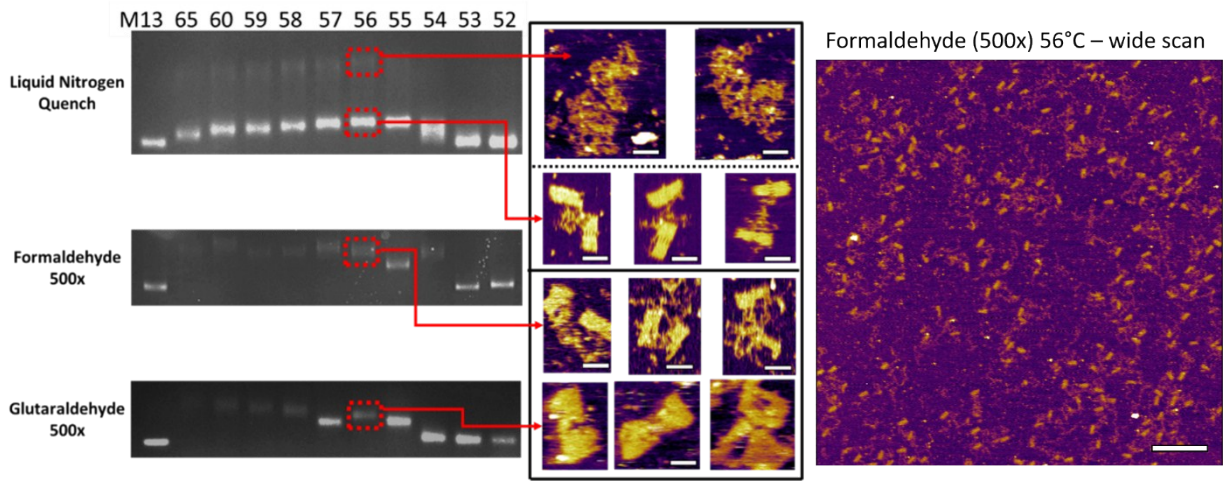

Figure S5. *Gel electrophoresis images showing the bands which were subjected to gel purification and the corresponding AFM images. Scale bars 50 nm*

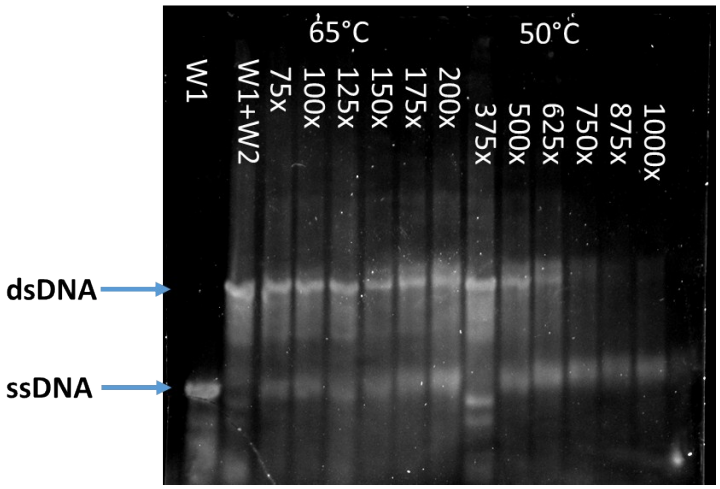

Figure S6*. PAGE Gel electrophoresis for quenching of two complementary ssDNA strands. Indicating that >200x excess is necessary for quenching at 65°C while ~750x was sufficient for quenching at 50°C*

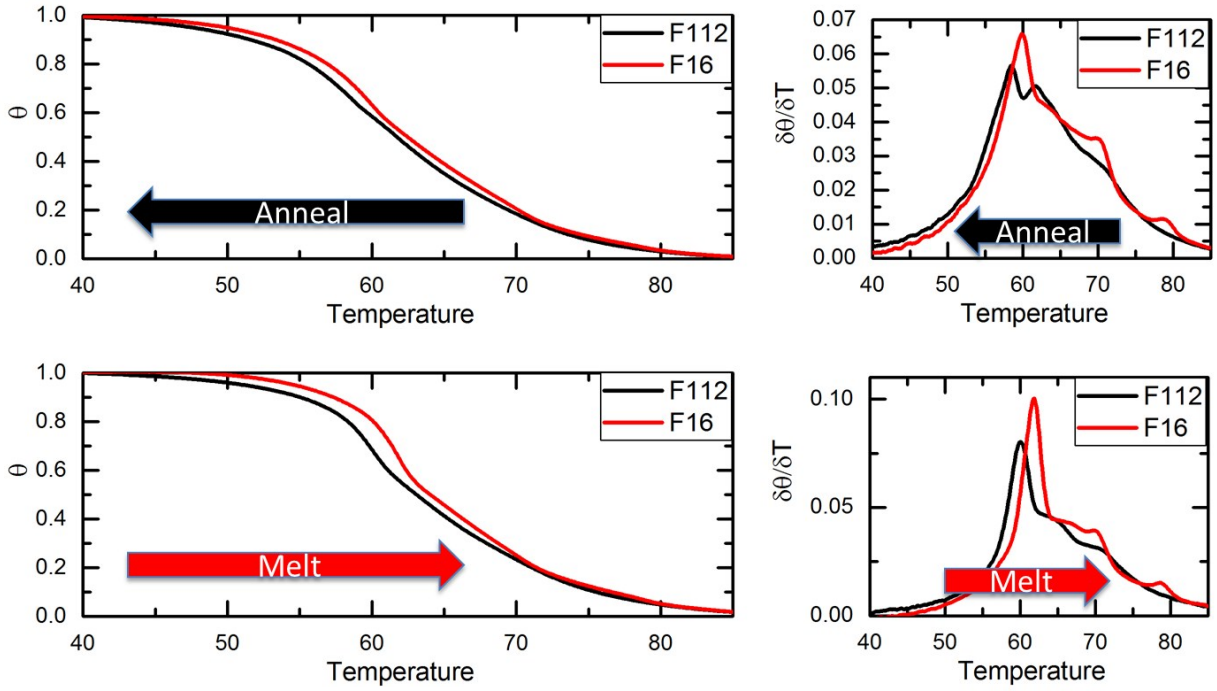

Figure S7. *Annealing and melting curves for F112 and F16 DNA origami where ϑ is the normalized fluorescence, or fraction of total formation, for the origami structures.*

Figure S7 shows the full melt and anneal curves for the F112 and F16 origami at 15 nM scaffold concentration and 10x staples. The curves shown were normalized as discussed in the methods using established protocols.[4] Figure S8 contains a table of design relevant values, staple motifs, routing pattern and GC content map for the F112 and F16. The routing map in Figure S8 is

	F112	F112 (v2)	F48	F16
Staple Motif	8-16-8	16-16	8-16-8	8-16-8
Scaff. Used	2240	2240	2304	2240
# Edge Staples	10	10	12	10
Staples 1/2 Crossovers	0	54	0	0
Staples Crossovers	54	0	44	4
Scaffold 1/2 Crossovers	0	0	0	0
Scaffold Crossovers	4	4	15	52
total 1/2 Crossovers	0	54	0	0
total Crossovers	58	4	59	56
Total Crossovers - Edge	47	-	-	47

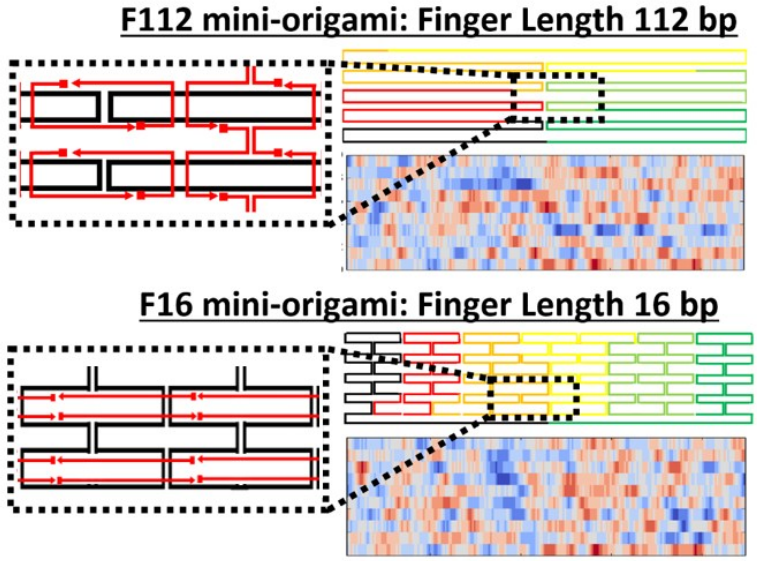

Figure S8: Table of design information, Staple motif, routing pattern and GC content map for F112 and F16. Table on right contains relevant information regarding the design of the F112, F16, and two alternate structures which were also considered.

colored in 400 bp segments of the scaffold so that the sequence of the yellow region is identical for both routings. From Figure S8, it can be seen that the staples for both structures have subsequences of 8 bp – 16 bp – 8 bp, although the staples in F112 jump in-between helices, while in F16 the scaffold jumps between helices while the staples stay within the same helix.
The table in Figure S8 indicates the staple motif, by the number base pairs in each subsequence, the total bases of scaffold strand used, the total number of edge staples, the total number of half and full crossovers in the structure divided by whether the staple or scaffold jumped helices, and the total number of crossovers. The final row, "Total Crossovers – Edge" are relevant for the F112 and F16. When annealed with edge staples, Figure 5 bottom left, they base stacked into rows. Quenches and anneal curves were performed without edge staples to make the structures more analogous and to make AFM images easier to interpret.
Quenches of F112 and F16 are shown in Figure S9. Lower quality AFM images in S9-A and higher quality AFM images were taken from separate, replicate experiments. Example image

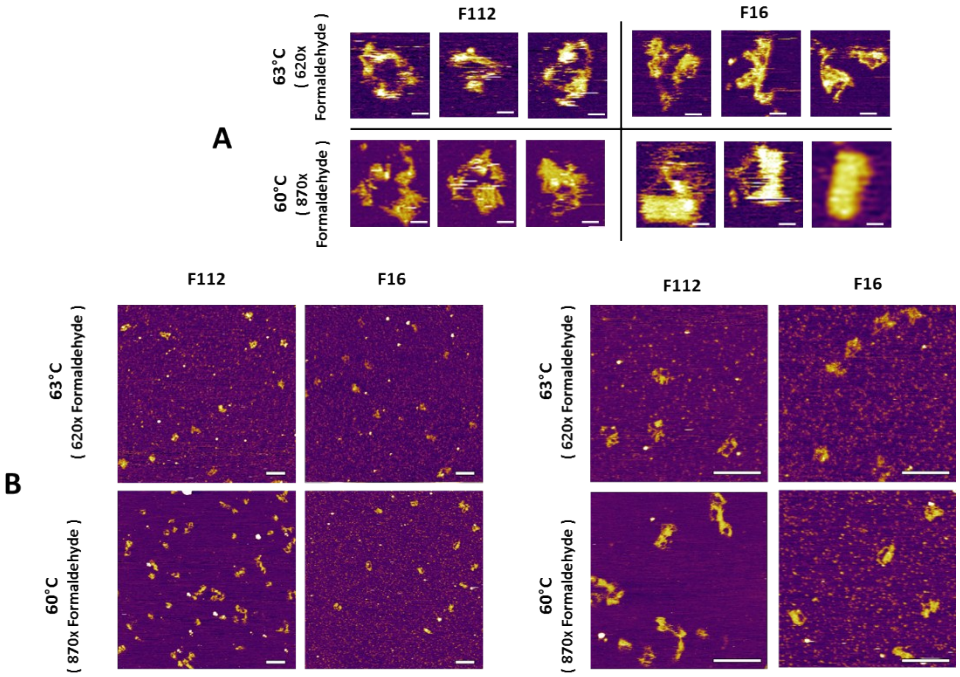

Figure S9: AFM images of two replicate sets of F112 and F16 quenches. Top scale bars 20 nm. Bottom scale bars 100 nm.

References

(1) Romano, K. P.; Newman, A. G.; Zahran, R. W.; Millard, J. T. *Chem. Res. Toxicol.* **2007**, *20* (5), 832.
(2) Rajendran, A.; Endo, M.; Katsuda, Y.; Hidaka, K.; Sugiyama, H. *J. Am. Chem. Soc.* **2011**, *133* (37), 14488.
(3) Garrett, E. R. *J. Am. Pharm. Assoc. (Scientific ed.)* **1960**, *49* (12), 767.
(4) Sanford, L. N.; Kent, J. O.; Wittwer, C. T. *Anal. Chem.* **2013**, 9907.